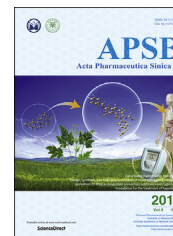




Chinese Pharmaceutical Association  
Institute of Materia Medica, Chinese Academy of Medical Sciences

Acta Pharmaceutica Sinica B

[www.elsevier.com/locate/apsb](http://www.elsevier.com/locate/apsb)  
[www.sciencedirect.com](http://www.sciencedirect.com)



REVIEW

# Development and application of hyaluronic acid in tumor targeting drug delivery



Zhijian Luo<sup>a,†</sup>, Yan Dai<sup>b,†,\*</sup>, Huile Gao<sup>c,\*</sup>

<sup>a</sup>Ultrasound Diagnosis Department of the Affiliated Hospital of Southwest Medical University, Southwest Medical University, Luzhou 646000, China

<sup>b</sup>Department of Pharmacy of the Affiliated Hospital of Southwest Medical University, Southwest Medical University, Luzhou 646000, China

<sup>c</sup>Key Laboratory of Drug Targeting and Drug Delivery System of the Education Ministry, Sichuan Engineering Laboratory for Plant-Sourced Drug and Sichuan Research Center for Drug Precision Industrial Technology, West China School of Pharmacy, Sichuan University, Chengdu 610041, China

Received 22 February 2019; received in revised form 8 May 2019; accepted 31 May 2019

## KEY WORDS

Hyaluronic acid;  
Tumor-active targeting;  
CD44;  
Tumor microenvironment;  
Reduction-sensitive;  
Enzyme-sensitive;  
Nanoparticles

**Abstract** Hyaluronic acid (HA) is a natural polysaccharide that has gained much attention due to its biocompatibility, enzyme degradation capacity and active tumor targeting capacity. Its receptor, CD44, is overexpressed in many kinds of cancers and is associated with tumor progress, infiltration and metastasis. Therefore, many researchers have developed various HA-based drug delivery systems for CD44-mediated tumor targeting. In this review, we systemically overview the basic theory of HA, its receptor and hyaluronidase, then we categorize the studies in HA-based drug delivery systems according to the functions of HA, including tumor-targeting materials, enzyme-sensitive biodegradable modality, pH-sensitive component, reduction-sensitive component, and the gel backbone. Finally, the perspective is discussed.

© 2019 Chinese Pharmaceutical Association and Institute of Materia Medica, Chinese Academy of Medical Sciences. Production and hosting by Elsevier B.V. This is an open access article under the CC BY-NC-ND license (<http://creativecommons.org/licenses/by-nc-nd/4.0/>).

\*Corresponding authors.

E-mail addresses: [daiyan@swmu.edu.cn](mailto:daiyan@swmu.edu.cn) (Yan Dai), [gaohuile@scu.edu.cn](mailto:gaohuile@scu.edu.cn) (Huile Gao).

<sup>†</sup>These authors made equal contributions to this work.

Peer review under responsibility of Institute of Materia Medica, Chinese Academy of Medical Sciences and Chinese Pharmaceutical Association.

<https://doi.org/10.1016/j.apsb.2019.06.004>

2211-3835© 2019 Chinese Pharmaceutical Association and Institute of Materia Medica, Chinese Academy of Medical Sciences. Production and hosting by Elsevier B.V. This is an open access article under the CC BY-NC-ND license (<http://creativecommons.org/licenses/by-nc-nd/4.0/>).

## 1. Introduction

Chemotherapy is still considered as one of the most commonly used and effective strategies to treat cancer. Unfortunately, the application of chemotherapeutics is shadowed by one or several shortages, including poor solubility of some drugs, low blood circulation time of one dose, limited tumor selection of formulations, and potentially severe drug-originated side effect. Thus, various nanotechnology-based drug delivery systems (DDSs) are developed to overcome the shortages of chemotherapeutics. Predominantly, the DDSs could passively target tumor by the enhanced permeability and retention (EPR) effect<sup>1,2</sup>. And specific ligands can be decorated onto the surface of DDSs to interact with receptors or proteins on the targeted cells, which could provide the DDSs with active targeting capacity<sup>3,4</sup>. Additionally, the DDSs could load a great variety of cargoes, such as photosensitizer, photothermal agent, immune regulator or stimulator, and radiation sensitizer, for enhanced synergistic combination therapy against solid tumors<sup>5,6</sup>.

For the development of novel DDSs, many materials are designed and synthesized with excellent properties, such as active targeting capacity, stimulus sensitivity, on-demand drug release and theranostic potential. However, a limited number of materials were approved by the FDA for the clinical application. Until now, only several nanomedicines have been approved for clinical application, such as Doxil<sup>®</sup>, paclitaxel albumin-bound nanoparticles (Abraxane<sup>®</sup>), paclitaxel PLA micelles (Genexol<sup>®</sup>), and paclitaxel-loaded liposomes<sup>7</sup>. What's worse, active targeting DDSs have not been approved yet, although there are several candidates under evaluation<sup>8</sup>. The most formidable barrier in the development of nanomedicine is the shortage of biocompatible

materials with excellent properties elucidated above. Therefore, many researchers have paid their attention to the natural degradable polymers.

Hyaluronic acid (HA) is a natural polysaccharide that consists of D-glucuronic acid and N-acetyl-D-glucosamine units. It is a linear polymer firstly discovered from bovine eyes in 1934, while the molecular weight ranges from thousands to millions Daltons depending on the length of the chain<sup>9</sup>. As a main component of extracellular matrix (ECM), HA is expressed in various organs, while the half distributes in skin<sup>10</sup>. Interestingly, HA is overexpressed in the tumor microenvironment, which shows complex biological activities. The cluster of differentiation (CD) protein, CD44, is considered as the main receptor of HA<sup>11</sup>, and the CD44–HA interaction is activated in many signaling pathways and involved in many biological processes, such as inflammation, wound healing, morphogenesis and cancer<sup>12</sup>. Furthermore, HA possesses good biocompatibility, easy modification, and enzyme degradation. Therefore, HA has gained much attention in cancer targeting drug delivery.

Although several reviews were published regarding the application of HA in DDSs<sup>9,13,14</sup>, none of which systemically over-viewed the application of HA in tumor targeting delivery, especially the different functions of HA in the tumor targeting DDSs. Therefore, in this review, we summarized the properties of HA and hyaluronidase expression, and then discussed the application of HA in tumor targeting delivery (Table 1), including as targeting delivery materials, constructing enzyme-sensitive nanoparticles, pH-sensitive nanoparticles, reduction-sensitive nanoparticles, and as backbone of gel. In the end, the concerns about current research and perspective were discussed.

**Table 1** The functions of HA in tumor targeting DDSs.

Function of HA		Typical DDS and mechanism
HA as tumor targeting ligand	Improving tumor cell targeting	HA was directly coated on the surface of DDS, and then targeted to CD44 on tumor cells <sup>15</sup> .
	Improving cancer stem cell targeting	CD44 expressed on tumor stem cells <sup>16</sup> .
	Reversing multidrug resistance	CD44-mediated endosome-involved internalization could bypass the Pgp and overcome MDR.
HA for controlled drug release	Improving macrophage targeting	CD44 was also expressed on macrophages <sup>17</sup> .
	Degradation by hyaluronidase	Degradation of HA by intracellular hyaluronidase could destroy the surface layer and trigger inner drug release <sup>18</sup> .
	Degradation by other enzymes	Drug-loaded gold nanoparticles (AuNPs) was coated with HA through cathepsin B-cleavable peptide (Gly-Phe-Leu-Gly-Cys) <sup>19</sup> .
HA for constructing enzyme sensitive nanoparticles	Dual stimuli sensitive drug release	The pores of nanoparticles was blocked by desthiobiotin and then coated with biotin-modified HA <sup>20</sup> . The drug release would be controlled by both biotin and hyaluronidase.
	Size changeable nanoparticles	Small sized nanoparticles were fabricated with HA to prepare size reducible nanoparticles <sup>21</sup> .
HA for constructing pH sensitive nanoparticles	Activatable imaging or treatment	Copper nanoparticles were coated with Cy5.5-decorated HA nanoparticles <sup>22</sup> . The fluorescence of Cy5.5 could be quenched by the nanoparticles and recovered when it was released.
	pH sensitive dissociation and release	pH sensitive units were modified onto the HA backbone for the preparation of pH sensitive nanoparticles <sup>23</sup> .
HA for constructing reduction sensitive nanoparticles	Reduction responsive dissociation and release	HA was conjugated to graphene oxide through disulfide bonds to endow the system with reduction sensitivity <sup>24</sup> .
HA as backbone of gel	Constructing nanogel and <i>in situ</i> gel	Methacrylate-modified HA and methacrylate-modified oxidized HA could be used as crossing precursors <sup>25</sup> .

## 2. Properties of HA, its receptors and hyaluronidase

### 2.1. Properties of HA

Several hydrophilic groups could be found in HA, including hydroxyl groups, carboxyl groups, and acetamido groups. These groups could form hydrogen bond intracellularly and provide the molecule with hydrophilicity and good solubility<sup>13,26</sup>. Additionally, the axial hydrogen atoms (C–H) in HA compose hydrophobic domain<sup>13</sup>, enabling HA to gain amphiphilic property, which is useful for the assembly of nanoparticles or micelles. The carboxyl groups in HA show a  $pK_a$  around 3–4, and can dissociate in the physiological condition<sup>14</sup>. Therefore, HA is one of negative-charged materials and can interact with extracellular cations, such as sodium ion, to form sodium hyaluronate. This property could be used for loading drugs or fabricating nanoparticles. For example, Liu et al.<sup>21</sup> directly mixed HA with cationic gold nanocluster (AuNC) to form nanoparticles, and doxorubicin (DOX) could be loaded into the nanoparticles simply by the electrostatic adsorption.

Except the targeting capacity, HA could improve the blood circulation time of nanoparticles. As we know, nanoparticles tend to form protein corona around them upon injection into the blood<sup>27,28</sup>. Normally, the formation of protein corona would facilitate reticular system clearance of nanoparticles, and the active targeting capacity of the nanoparticles may be suppressed due to protein corona<sup>29–31</sup>. Of note, HA provides an alternative solution to reduce protein absorption and decrease the immunogenicity of NPs, apart from commonly used polyethylene glycol (PEG)<sup>32,33</sup>. Compared with uncoated chitosan nanoparticles, the protein absorption fell by about 2.5 times in HA-coated counterparts. Therefore, HA coatings could effectively prolong blood circulation time and biocompatibility.

HA itself plays a significant role in many processes, including embryonic development, wound healing, regeneration, and repair<sup>34</sup>. It also contributes significantly to the cancer progression. The accumulation of HA in tumor stroma could modulate tumor cell proliferation, motility and invasiveness, and it also acts as a regulator during the angiogenesis<sup>35,36</sup>. Therefore, the high level of HA, even its low molecular fragment, is considered as a biomarker of tumors malignancy<sup>37</sup>.

### 2.2. Properties of HA receptors

CD44 is considered as the most widely studied receptor of HA. CD44 is a transmembrane glycoproteins family that contains variant isoforms. The standard isoform, CD44s, is ubiquitous, while the variant isoform, CD44v, is mainly overexpressed in cancer cells. The CD44v in cancer displays elevated HA binding, resulting in increased tumorigenicity<sup>36</sup>. CD44v6, a specific isoform of CD44v, is considered as the main receptor overexpressed in many kinds of cancers, while it does not express in normal tissues<sup>38</sup>. The expression level of CD44v6 is considered associated with the progression of tumor. Furthermore, the CD44 in cancer stem cells has self-renewal capacity<sup>39,40</sup>, and it shows high level on many kinds of tumor stem cells, which improves the motility of the stem cells<sup>16,41,42</sup>. So these properties make HA an excellent targeting material for drug delivery. The CD44 is also expressed on macrophages, and several studies<sup>43,44</sup> developed HA-based nanoparticles for the targeting delivery to tumor-associated macrophages, which repolarized the M2 type to M1 type and reversed the immunosuppressive condition in tumor.

CD168, previously known as receptor of hyaluronan-mediated motility (RHAMM), is one of receptors of HA and is overexpressed in human tumors. The CD168 is associated with the high metastasis and poor survival rate<sup>45–47</sup>. Other receptor, such as HA receptor for endocytosis (HARE), can bind with not only HA, but also heparin, dermatan sulfate, acetylated LDL, and apoptotic debris, and boost their elimination from the circulation<sup>48</sup>. The HARE shows size-dependent binding affinity with HA. It can bind with HA in a molecular weight ranging 40–400 kD, while others can not<sup>49</sup>.

### 2.3. Properties of hyaluronidases

Hyaluronidases, the enzymes to degrade HA, are expressed in many tissues<sup>50</sup>. In human, there are six kinds of hyaluronidases, *i.e.*, HYAL-1, HYAL-2, HYAL-3, HYAL-4, PH-20/SPAM1 and PHYAL<sup>34</sup>. Most members of the hyaluronidase family are involved in the tumor process<sup>51</sup>. In several tumors, hyaluronidase is demonstrated with high expression level<sup>52,53</sup>. While the expression level in metastasis is even higher than that in the primary tumor<sup>54</sup>, and the high level of hyaluronidase is also associated with malignancy of tumor<sup>55</sup>. Therefore, the hyaluronidase could be used as stimulus to degrade the HA-based DDSs.

## 3. HA in tumor-targeting drug delivery

### 3.1. HA as tumor-targeting ligands

#### 3.1.1. Improving tumor cell targeting

Tumor cell-overexpressed CD44 targeting is a most widely used function of HA. Direct conjugation drugs onto HA could form CD44 targeting polymer drug conjugates, which was easy to prepare. HA and paclitaxel (PTX) conjugate (ONCOFID<sup>TM</sup>-T) was under phase II clinical trial evaluation to treat bladder and ovarian cancers<sup>56,57</sup>. When it comes to combination therapy, incubating MDA-MB-231 cells with gemcitabine (GEM) for 24 h prior to DOX displayed markedly higher synergistic outcomes than simultaneous incubation<sup>58</sup>. Therefore, Vogus et al.<sup>58</sup> conjugated DOX and GEM onto the HA backbone (DOX-GEM-gly-HA) for the synergistic treatment of triple negative breast cancer. Then the release of GEM from DOX-GEM-gly-HA was much faster than DOX at both pH 5.0 and 7.4, which was suitable to maximize the synergy of GEM and DOX. *In vivo*, the DOX-GEM-gly-HA (2 mg/kg DOX and 2.75 mg/kg GEM) significantly inhibit the tumor growth, with a higher tumor inhibiting effect than the single drug-loaded polymers. After 4 times' injection (every 3 days), the tumor size of DOX-GEM-gly-HA group was only 68 mm<sup>3</sup>, while the control group was bigger than 500 mm<sup>3</sup>. The HA prodrug could be coated onto particles for tumor actively targeting drug delivery. Lv et al.<sup>59</sup> modified paclitaxel (PTX)—HA prodrug onto marimastat (MATT)-loaded thermal-sensitive liposomes to deliver drugs towards both tumor cells and tumor microenvironment. At 42 °C, the hybrid nanoparticles (HA-PTX/MATT-LTSL HNPs) showed much faster release than that at 37 °C. *In vivo*, the dye-loaded particles (HA-PTX/DiR-LTSL HNPs) showed higher fluorescent intensity in 4T1 tumor than the particles without HA coating (DiR-LTSLs) (Fig. 1), demonstrating that HA coating improved tumor targeting capacity of nanoparticles. After staining tumor vessels, it showed that the particles could enter both tumor cells and tumor microenvironment, and that the particles remained stable because of the colocalization of fluorescence of both Rho-HA-PTX and CF-LTSLs (Rho and CF

are fluorescent dyes). Consequently, the loaded MATT significantly inhibited the expression and activity of matrix metalloproteinase, and the expression of TGF- $\beta$ 1, while PTX effectively induced tumor cell apoptosis. As a result, the particles significantly hampered 4T1 tumor growth, metastasis and tumor cell angiogenesis.

Coating nanoparticles with HA could form a HA surface layer, which could improve biocompatibility, blood circulation time, and most importantly, active targeting capacity mediated by CD44 overexpressed on many cancer cells<sup>9,13</sup>. For example, coating the curcumin-loaded zein nanoparticles with HA could also effectively deliver curcumin into CD44-overexpressed CT26 tumor cells, improving the drug distribution in tumor and enhancing antitumor effect<sup>15</sup>. Coating nanoparticles with HA is another commonly used strategy for CD44-targeting drug delivery. Zhang et al.<sup>60</sup> coated cytarabine and IR820-loaded zeolitic imidazolate framework-8 (ZIF-8) with HA for the tumor targeting chemophotothermal therapy. The HA coating considerably increased 4T1 cell uptake, and the IC<sub>50</sub> decreased 1.5 times compared with the drug-loaded MOF without HA coating. Wang et al.<sup>61</sup> fabricated a kind of oxygen-deficient molybdenum oxide (MoO<sub>3-x</sub>)-hybridized HA nanoparticles, which showed CD44-active targeting photothermal therapy accompanied with photoacoustic imaging capacity. Similarly, coating WS<sub>2</sub> nanodots with polyaniline and HA significantly improved the tumor-targeted photothermal and photodynamic therapy<sup>62</sup>, which was attributed to the specific interaction between HA and tumor overexpressed HA. Modifying the HA-coated DDSs with other ligands could further improve tumor targeting capacity. Although active targeting capacity is one of the most commonly used functions of HA, the interaction between HA and CD44 is influenced by the molecular weight of HA<sup>14</sup>, which should be taken into consideration when constructing HA-based tumor targeting DDSs.

### 3.1.2. Improving cancer stem cell targeting

The HA coating or modification could be used to target tumor stem cells because of the overexpression of CD44 on the tumor stem cells<sup>16</sup>. Shen et al.<sup>63</sup> coated solid lipid nanoparticles (SLNs) with HA (HA-SLNs) for targeting delivery of PTX to melanoma stem-like cells. It showed that the melanoma stem-like cells expressed high level of CD44 while normal cancer cells expressed low level. *In vitro*, the PTX-loaded HA-SLNs showed higher cellular uptake in stem-like cells and induced higher percentage of apoptosis cells than the PTX-loaded SLNs. Furthermore, the PTX-

loaded HA-SLNs significantly inhibited the formation of spheroids. *In vivo*, the PTX-loaded HA-SLNs significantly decreased the growth of tumor, which was better than other particles and free drug. Similarly, Marengo et al.<sup>64</sup> loaded diethyldithiocarbamate-copper into HA-decorated liposomes for targeting pancreatic cancer stem cells. The results showed the HA-decorated liposomes effectively improved the cellular uptake, and significantly inhibited the proliferation of the cells.

### 3.1.3. Reversing multidrug resistance (MDR)

Tumor MDR involves several mechanisms<sup>65</sup>, while the overexpression of MDR transporters, especially P-glycoprotein (Pgp), is considered as the primary reason. HA could bind with CD44 receptors and mediate endosome-involved internalization, which helps bypass the Pgp and overcome MDR. Docetaxel (DTX) and disulfonated tetraphenyl chlorin (TPCS2a) were co-loaded into poly (lactide-co-glycolide) (PLGA) and PEI nanoparticles for the combination of chemotherapy and photodynamic therapy, and the nanoparticles were coated with HA (DTX/TPCS2a-NPs) for tumor targeting delivery<sup>66</sup>. In the DTX-resistant HeLa cell line (HeLa-R), the IC<sub>50</sub> of DTX increased 8-fold from 0.011  $\mu$ g/mL in parent HeLa cells (HeLa-P) to 0.093  $\mu$ g/mL, and the membrane efflux pumps, such as the Pglycoprotein (P-gp), were overexpressed. After drug loading into the particles, DTX-NPs showed much higher antitumor effect than free DTX. While the DTX/TPCS2a-NPs showed a much lower CI value in HeLa-R cells than in HeLa-P cells, demonstrating the HA could effectively improve the targeting delivery of drugs to resistant tumor cells.

Although the CD44 involved internalization could bypass Pgp and deliver drugs into cells, the MDR transporters still could pump out the drugs. Therefore, co-delivery transporter inhibitors would be promising in overcoming MDR. D- $\alpha$ -Tocopheryl PEG 1000 succinate was an effective Pgp inhibitor<sup>67</sup>, so Zhang et al.<sup>68</sup> developed a cathepsin B-activatable PTX prodrug-loaded  $\alpha$ -tocopherol succinate-modified chitosan nanoparticles, and then coated them with HA-PEG. At pH 5.0 and in the presence of cathepsin B, the nanoparticles released about 80% PTX after 128 h incubation. In contrast, the release was only about 20% without cathepsin B. In the PTX resistant MDA-MB-231 cells (MDA-MB-231/PTX), the HA coating clearly elevated the cellular uptake after 24 h incubation. Consequently, the particles induced highest tumor cell apoptosis and the expression of P-gp was lowest, demonstrating the particles could effectively target and reverse multidrug resistance. Additionally, HA coated gold

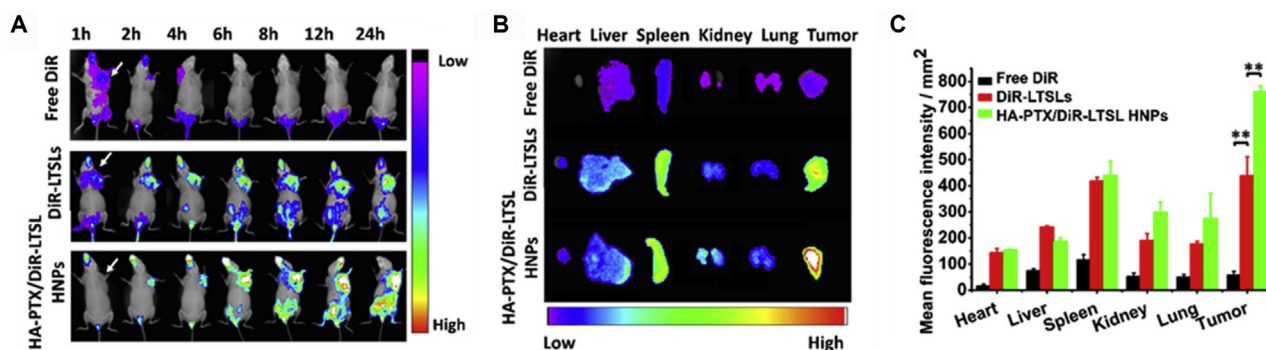


**Figure 1** *In vivo* tumor targeting of HA-coated hybrid nanoparticles. Whole body imaging (A), organ imaging (B) and semi-quantitative fluorescent intensity (C) demonstrated the HA coating significantly improved tumor targeting capacity of nanoparticles. Reprinted from Ref. 59 with permission. Copyright © 2018 American Chemical Society.

nanorods could be used for overcoming resistance to DOX because the hyperthermia generated by laser irradiation of gold nanorods could suppress the drug efflux process and enhance tumor cell apoptosis<sup>69</sup>.

### 3.1.4. Improving macrophage targeting

The CD44 was also expressed on macrophages, enabling HA with the capacity of targeting delivering drugs to tumor associated macrophages to repolarize them from M2 type to M1 type<sup>17</sup>. Noncoding micro-RNAs (miR), such as miR-29, miR-125, and miR-155, could promote the TAM from M2 type to M1 type, thus enhancing the immune response and antitumor effect<sup>43</sup>. Parayath et al.<sup>17</sup> encapsulated miR-125b into HA-poly (ethyl-amine) (HA-PEI) based nanoparticles (Fig. 2). After intraperitoneal administration, the particles could be selectively taken up by F4/80<sup>+</sup> peritoneal macrophages, indicating a good macrophage targeting capacity. After loading with miR-125b, the nanoparticles (HA-PEI-miR-125b) significantly increased the M1 to M2 macrophage ratio, which was 6-fold higher than the control. Comparably, the iNOS (M1 maker)/Arg-1 (M2 maker) ratio was increased over 300-fold in the TAMs after treatment. These results clearly demonstrated the HA-PEI could effectively deliver miR-125b to macrophages and repolarize TAM from M2 to M1, leading to an enhanced immunotherapy to nonsmall cell lung cancer.

## 3.2. HA for controlled drug release

### 3.2.1. Degradation by hyaluronidase

The deshielding and drug release could be also achieved by degradation of HA by intracellular hyaluronidase. Monocarboxylate

transporter 1 (MCT1) is responsible for the tumor cell survival because of its capacity in facilitating lactate uptake<sup>70</sup>, while the lactate-fueled respiration consumes much oxygen and leads to low intracellular oxygen concentration and poor response to photodynamic therapy<sup>71</sup>. To improve the photodynamic therapy and anti-tumor effect, Chen et al.<sup>18</sup> loaded MCT1 inhibitor  $\alpha$ -cyano-4-hydroxycinnamate (CHC) into porous Zr (IV)-based porphyrinic metal-organic framework (PZM) nanoparticle and then coated the nanoparticle with HA. The HA could actively target tumor cells and trigger internalization. Then HA was degraded by the hyaluronidase and the CHC was released to inactivate MCT1, which would improve the photodynamic therapy of the PZM nanoparticle (Fig. 3). In comparison with hyaluronidase-free medium, CHC release in the presence of 0.1 mg/mL hyaluronidase medium increased from 10% to 65% within 24 h.

Chen et al.<sup>72</sup> coated graphene oxide (GO)—ZnO nanoparticles with HA to improve the biocompatibility, colloid stability and tumor targeting capacity. Moreover, the fluorescent molecule-labeled HA could be degraded by hyaluronidase-1 after CD44-mediated tumor cell internalization, thus detached from GO and the fluorescence of the FITC was recovered, which could be used for tracking the internalization of the nanoparticles. He et al.<sup>73</sup> loaded H<sub>2</sub>O<sub>2</sub> activated RNase and photosensitizer in acid-degradable polyethyleneimine (PEI)-based nanoparticles and then coated them with HA. The HA could mediate the long blood circulation time, tumor targeting delivery and CD44 involved internalization. Then the particles could escape from the endosomes due to the protonation of PEI, and HA could be degraded to deshield. Upon laser irradiation, the photosensitizer would produce ROS and then activate RNase for the induction of tumor cell apoptosis.

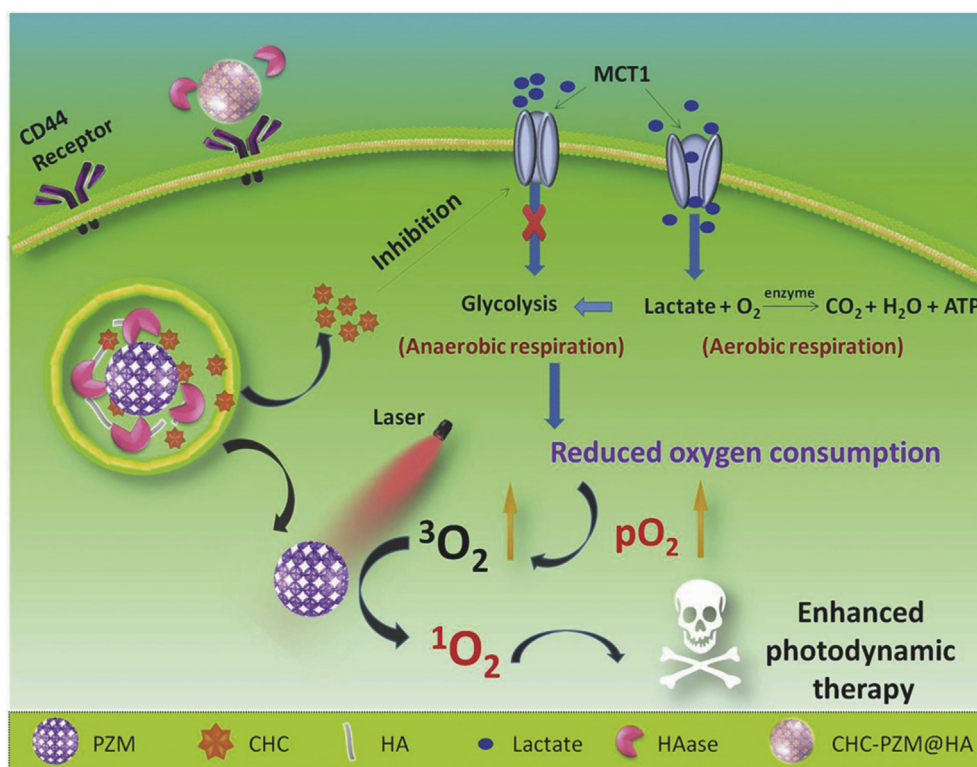


**Figure 2** Schematic representation of intraperitoneal administration of hyaluronic acid-poly(ethylene imine) (HA-PEI)—microRNA 125b. Reproduced from Ref. 17 with permission. Copyright © 2018 American Chemical Society.

### 3.2.2. Degradation by other enzymes

Coating nanoparticles with HA through specific linkers may achieve controlled deshielding and drug release. Gotov et al.<sup>19</sup> coated DTX-loaded gold nanoparticles (AuNPs) with HA through cathepsin B-cleavable peptide (Gly-Phe-Leu-Gly-Cys; GFLGC). HA could improve the targeting capacity of the nanoparticles, and it can be detached from the surface of AuNPs in tumor cell endosomes because of the high level of cathepsin B, leading to burst release of DTX and high antitumor effect. Although authors demonstrated the responsivity to cathepsin B, the HA on the nanoparticles may be degraded by the intratumor hyaluronidase, and trigger premature drug release.

### 3.2.3. Dual stimuli sensitive drug release

Additionally, the deshielding and drug release could be controlled by both hyaluronidase and other stimuli. Zhang et al.<sup>20</sup> loaded chemotherapeutic DOX into the pores of the mesoporous silica nanoparticles (MSN), blocked the pores by desthiobiotin-streptavidin and then coated them with biotin-modified HA to render the particles with tumor targeting capacity. In the presence of both biotin and hyaluronidase, the DOX could be released over 80% at 24 h. In comparison, the release with only one stimulus, biotin or hyaluronidase, was about 60% or 40%, respectively, while the release further decreased to only 12% without both stimuli. The results clearly demonstrated the release was gated by both biotin and hyaluronidase. In both colon-26 and HT-29 cells, the particles (MSN-HA/DOX) could be taken up with high intensity, and the addition of free HA would reduce the cellular uptake, indicating the CD44-involved internalization. *In vivo*, the MSN-HA/DOX treated group showed the lowest tumor growth rate, while the tumor tissues showed highest apoptosis according to TUNEL and H&E staining. The study provided a sequential control of drug release, which would be useful for improving the selectivity of DDSs.

## 3.3. HA for constructing enzyme sensitive nanoparticles

### 3.3.1. Size changeable nanoparticles

The particle size could greatly influence the penetration and retention of nanoparticles in tumor<sup>74–76</sup>. Normally, particles with small size could easily enter inner part of tumor, but also easily backflow to vessels; while particles with large size display good retention capacity, but they tend to distribute near blood vessels rather than penetrate into the tumor part that is distant from tumor microvessels<sup>77–79</sup>. Therefore, to satisfy the controversial requirement of the particle size, several researchers developed size-changeable nanoparticles that can response various tumor microenvironment stimuli, such as enzymes, light, pH, etc.<sup>80–83</sup>. Hyaluronidase is overexpressed in most of tumors<sup>84,85</sup>, thus the corresponding substrate, HA, could be used for the constructing of hyaluronidase responsive size changeable nanoparticles.

Our group firstly fabricated small-sized cationic bovine serum albumin-protected AuNCs (AuNCs@CBSA, about 8 nm) with negative charged HA to form nanoparticles (AuNC@CBSA-ICG@HA), while the photothermal agent indocyanine green (ICG) was loaded into the particles directly during nanoparticle formation<sup>86</sup>. The particle size of AuNC@CBSA-ICG@HA was 201.9 nm, which can decrease to about 50 nm in the presence of hyaluronidase, indicating that the AuNC@CBSA-ICG@HA could undergo enzyme-sensitive size change. According to the *in vitro* penetration through 4T1 tumor spheroids, incubating AuNC@CBSA-ICG@HA with hyaluronidase before the treatment

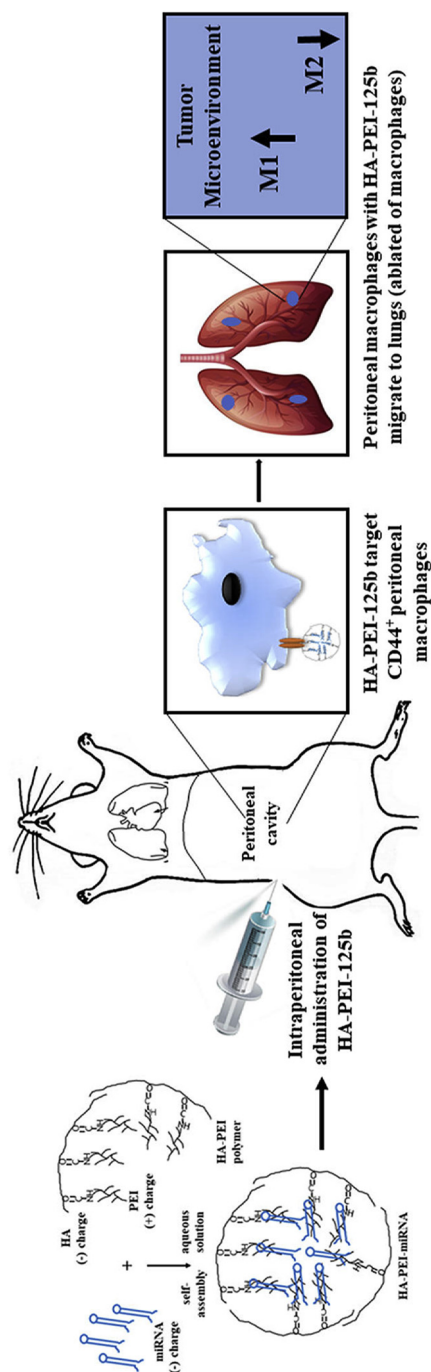


**Figure 3** Schematic illustration of the interfering with the lactate-fueled respiration for enhanced photodynamic tumor therapy by a porphyrinic MOF nanopatform. Reprinted from Ref. 18 with permission. Copyright © 2018 Wiley.

with tumor spheroids could greatly enhance the penetration into the core of spheroids (Fig. 4). As a result, the *in vivo* tumor accumulation of AuNC@CBSA-ICG@HA was about 2.5-fold higher than that of AuNC@CBSA-ICG with smaller size. Due to the higher retention and penetration of AuNC@CBSA-ICG@HA in tumor, the temperature of tumor after laser irradiation could achieve as high as 77.8 °C, which was much higher than that of AuNC@CBSA-ICG (62.4 °C).

To further improve the tumor targeting capacity, nitric oxide (NO) was introduced into the HA-based nanoparticles because the NO could open the endothelial cell junction gaps and enhance the

tumor EPR effect<sup>87</sup>. The NO-incorporated paclitaxel (PTX) and ICG-loaded nanoparticles, AuNC@CBSA-PTX-ICG@HA-NO<sub>3</sub>, could also be degraded by hyaluronidase and led to size reduction<sup>21</sup>. Furthermore, the particles could quickly release NO in the presence of glutathione (GSH). The concentration of NO after 24 h incubation with GSH could achieve 1000 nmol, while the concentration was only 300 nmol without the presence of GSH. In comparison with the particles without NO donor, AuNC@CBSA-PTX-ICG@HA-NO<sub>3</sub> showed higher cellular uptake and penetration through 4T1 tumor spheroids. Consequently, the particles led to the highest percentage of tumor cell apoptosis and the best

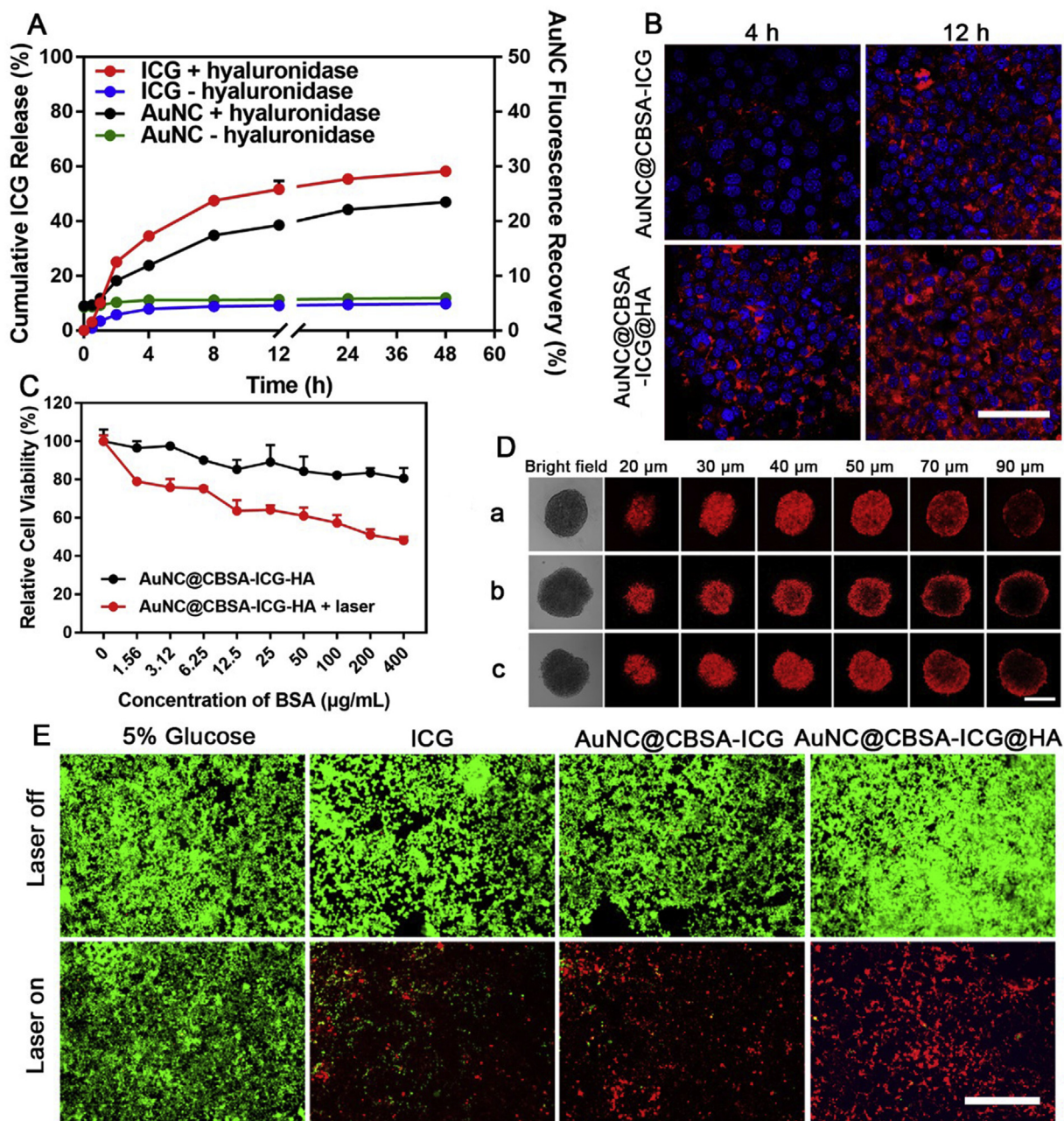


**Figure 4** (A) Cumulative ICG release and fluorescence recovery with or without hyaluronidase through release procedure. (B) Cellular uptake of nanoparticles after incubation for 4 and 12 h. The white bar represents 50 μm. (C) Cell viability measured by MTT assays. (D) Nanoparticles penetrating into tumor spheroids. The white bar represents 200 μm. (a) represents AuNC@CBSA-ICG, (b) represents AuNC@CBSA-ICG@HA and (c) represents AuNC@CBSA-ICG@HA pretreated with hyaluronidase. (E) The *in vitro* photothermal effect of formulations measured by Calcein-AM/PI double staining. The white bar represents 200 μm. Reproduced with Ref. 86 with permission of Gao et al.

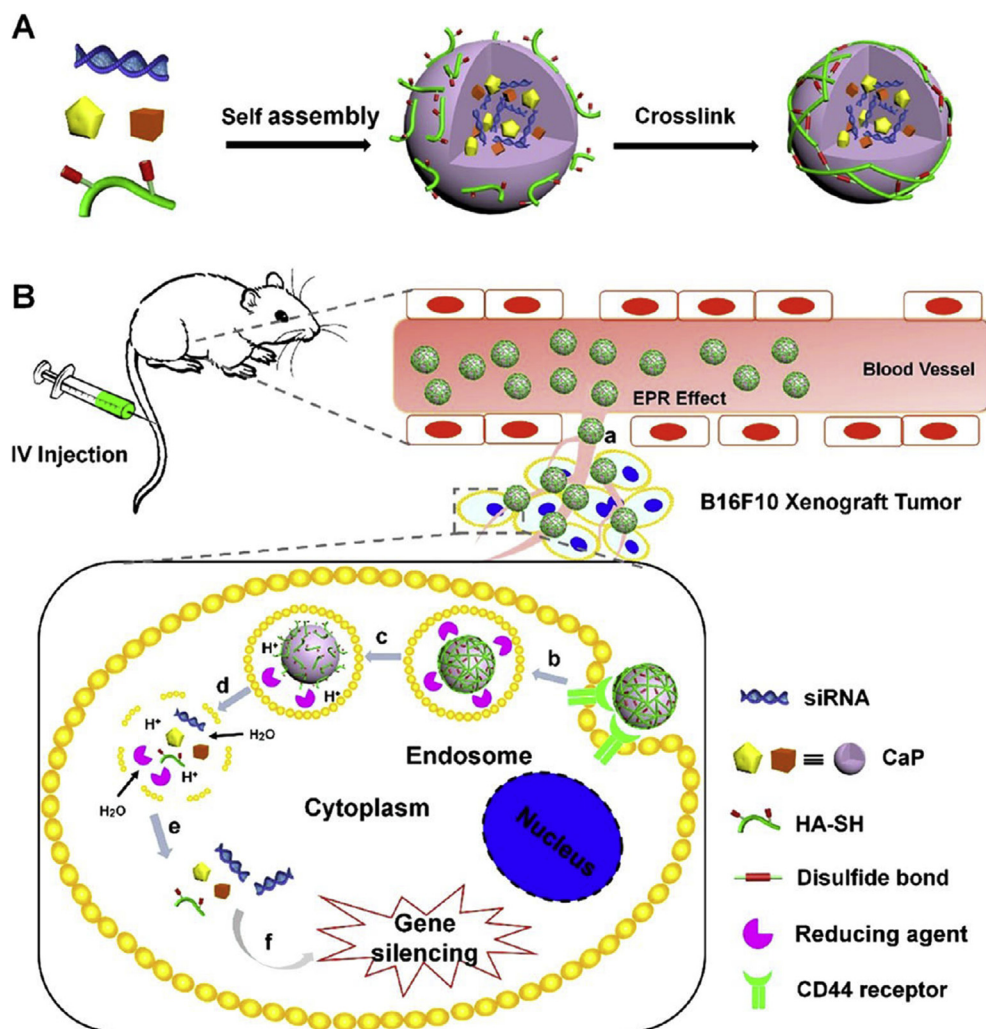


**Figure 5** (A) Schematic illustration of a cross-linked anionic delivery system, consisting of siRNA-loaded HA-SH/CaP hybrid nanoparticles (NPHA-SH/CaP/siRNA); (B) schematic illustration of tumor-targeted siRNA delivery by HA-SH/CaP nanoparticles. Reproduced with permission from Ref. 105. Copyright © 2017 American Chemical Society.

antitumor effect. The size-shrinkable strategy could also be applied in dendrimer–HA-fabricated nanoparticles, which showed similar results as regards tumor penetration, retention and antitumor effect<sup>88</sup>. The coadministration of iRGD with particles could further improve targeting capacity relative to the sole dendrimer–HA-fabricated nanoparticles, due to the effect of iRGD on improving vascular and tissue permeability in a tumor-specific and neuropilin-1-dependent manner.<sup>89,90</sup>

The size-changeable capacity could also be achieved by the response to other stimuli, such as matrix metalloproteinase-2 (MMP-2) and legumain<sup>91,92</sup>. Han et al.<sup>93</sup> fabricated small sized poly (amidoamine) (PAMAM) with HA through MMP-2 sensitive peptide (PLGLAG) to get a 200 nm nanoparticle HA-pep-PAMAM. After incubation with MMP-2 for 4 h at pH 7.4, the size of DOX-loaded HA-pep-PAMAM (HA-pep-PAPAM/DOX) greatly decreased from 200 nm to about 10 nm, whereas no significant change was observed in the control nanoparticles without MMP-2-sensitive peptide linker (HA-PAMAM), indicating that the PLGLAG peptide could provide nanoparticles with MMP-2-sensitive size-shrinkable capacity. *In vitro*, the shrinkable HA-pep-PAMAM/DOX showed greater penetration in A549 tumor

spheroids. Consequently, the HA-pep-PAPAM/DOX showed enhanced tumor localization and antitumor effect.

### 3.3.2. Activatable imaging or treatment

The hyaluronidase degradation capacity of HA could also be used for activatable imaging and treatment. Zhang et al.<sup>22</sup> loaded copper nanoparticles (CuS) into Cy5.5-decorated HA nanoparticles (HANPC). The fluorescence of Cy5.5 could be quenched by CuS nanoparticles. But when they targeted to tumor, the overexpressed hyaluronidase could degrade HA and release CuS and Cy5.5, then the fluorescence was recovered, making it capable of monitoring intratumor distribution of nanoparticles. After laser irradiation, the CuS nanoparticles could transfer light to heat, and the temperature could achieve about 90 °C *in vitro* and 50 °C *in vivo*, leading to effective photothermal therapy and a high tumor inhibition rate of 89.7%. Additionally, the released Cy5.5 could be used for both fluorescent imaging and photoacoustic imaging, resulting in a tumor-to-normal tissue ratio of 3.25 and 3.8, respectively. Attaching AuNCs directly onto HA could also construct enzyme-activatable nanoparticles. Han et al.<sup>94</sup> produced a kind of verteporfin-loaded gold nanoclustered HA nanoparticles

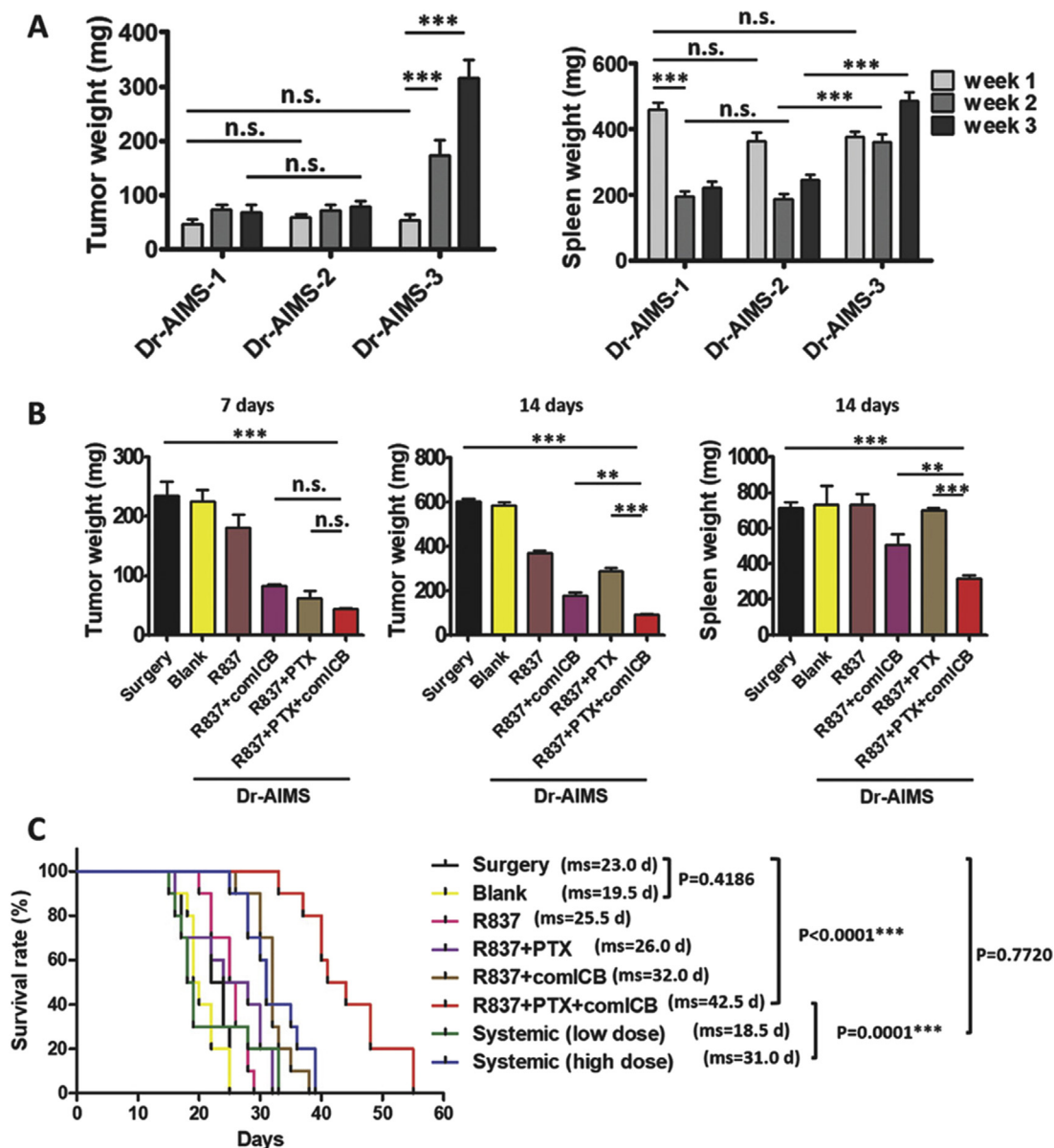


**Figure 6** The comparison of tumor weight and spleen weight (A and B) at different intervals. Then the survival curve after treatment was recorded (C). \* $P < 0.05$ , \*\* $P < 0.01$ , \*\*\* $P < 0.001$ . The Dr-AIMS treatment effectively modulated the immunosuppressive TME and further enhanced therapeutic efficacy of immunotherapy. Reprinted from Ref. 25 with permission. Copyright © 2018 Wiley.

(GNC-HyNA) for photothermal therapy and activated photodynamic therapy. In circulation, the AuNCs surface protected the verteporfin from light irradiation and reduced the toxicity. After actively targeting MDA-MB-231 tumor, laser irradiation led to hyperthermia and disassociation of the nanoparticles, while hyaluronidase could degrade HA and further improved the disassociation. Then the verteporfin was released and further laser irradiation would produce high level of ROS, resulting in effective photodynamic therapy.

### 3.4. HA for constructing pH sensitive nanoparticles

Due to the anaerobic glycolysis in tumor, tumor microenvironment showed lower pH value than physiological condition, commonly 6.0–6.8 in the tumor matrix. Therefore, pH-sensitive

nanoparticles could be designed with good tumor cell internalization, penetration and responsive drug release<sup>95,96</sup>. To introduce pH sensitive property to HA, Miyazaki et al.<sup>23</sup> modified 3-methyl glutarilated (MGlu) units or 2-carboxycyclohexane-1-carboxylated (CHex) units onto the HA backbone. The  $pK_a$  of carboxyl groups in HA is reported as 3.04, while modification with MGlu and CHex changed the  $pK_a$  to 5.4–6.7, indicating these HA derivates could be protonated in the tumor microenvironment. Then the MGlu–HA and Chex–HA were used to modify liposomes by directly adding lipid during liposome preparation. In neutral pH, the pyranine was retained in the liposomes without apparent leakage. In contrast, the pyranine was released in 10 min from MGlu–HA- and Chex–HA-modified liposomes, while HA-modified liposomes only showed slight content release, demonstrating the modification with MGlu–HA

and Chex-HA could provide pH-sensitive drug release property. Correspondingly, the Chex-HA-modified liposomes could specifically interact with CD44-overexpressed Hela and colon26 cells, resulting in higher cellular uptake, rapid intracellular drug release and better antiproliferation effect.

The pH sensitivity could be introduced by the application of coiled-coil peptide. Ding et al.<sup>97</sup> conjugated coiled-coil peptide (E3 or K3) with HA to form nanogels with pH sensitivity. The nanogels were stable at pH 7.4, showing a particle size of 176 nm. In pH 7.4, only 18.4% of the loaded protein drug saporin remained after 24 h incubation. Interestingly, the 24 h drug release increased to 76.8% and 85% at pH 6.0 and 5.0, respectively. Consequently, the nanogels showed higher MCF-7 cell uptake and intracellular protein release, significantly improving antitumor effect *in vitro*.

### 3.5. HA for constructing reduction sensitive nanoparticles

Graphene oxide (GO) has attracted great attention in drug delivery and bioimaging. But the *in vivo* application of GO was shadowed by the aggregation potential and instability. Therefore, many studies modified GO with various compounds to improve the stability and targeting capacity. Yin et al.<sup>24</sup> modified GO with HA to improve the physiological stability and CD44-oriented tumor actively targeting. To endow the system with reduction sensitive de-shielding and drug release, the HA was conjugated to GO through disulfide bonds (HSG). What's more, the deshielding of HA in the high level of intracellular GSH could lead to burst release of DOX, resulting in improved antitumor effect. In comparison to the undetachable particles (DOX-loaded HA-modified GO through adipic dihydrazide, HCG-DOX), the half-maximal inhibitory concentration (IC<sub>50</sub>) of redox-sensitive particles (HSG-DOX) on MDA-MB-231 cells decreased from 1.89 to 1.5 µg/mL. When combined with NIR irradiation, the IC<sub>50</sub> of HSG-DOX could further decrease to 0.55 µg/mL, but the IC<sub>50</sub> of HCG-DOX increased to 7.60 µg/mL. *In vivo*, the HSG-DOX plus NIR irradiation showed best antitumor effect, which was better than the HSG-DOX and HSG-DOX plus NIR. Similarly, conjugating HA with tocopherol succinate (TOS) through disulfide bond could obtain an amphipathic molecule HA-ss-TOS, which could be assembled into micelles and loaded with chemotherapeutic PTX<sup>98</sup>. The micelles (HA-ss-TOS/PTX) could release PTX much faster in the presence of 20 mmol/L GSH than without GSH and the micelles without disulfide bond, demonstrating the reduction-sensitive drug release profile. *In vitro*, the micelles could be effectively taken up by B16F10 cells, leading to greater cell apoptosis. Consequently, the micelles showed higher tumor accumulation and better tumor inhibition *in vivo* than the uncleavable controls. Conjugating HA with other polymers through disulfide bond, such as poly (lactide) (PLA)<sup>99</sup>, pyrenyl<sup>100</sup>, 6-mercaptopurine<sup>101</sup>, vitamin E succinate<sup>102</sup>, and curcumin<sup>103</sup>, were all utilized for reduction sensitive drug delivery.

Coating particles with disulfide cross-linked HA (HA-ss-HA) could also achieve reduction sensitive release. Zhou et al.<sup>104</sup> condensed siRNA by positive calcium phosphate (CaP) and then coated the core with HA-ss-HA for tumor active targeting delivery and intracellular release of siRNA (Fig. 5). Incubating the nanoparticles with 10 mmol/L of GSH could cause the disruption of the spherical morphology *in vitro*. In B16F10 cells, the uptake of the nanoparticles could be greatly inhibited by the free HA, indicating the HA-mediated cellular internalization. The siRNA could effectively escape from cell endosomes due to the high level of intracellular GSH, while the escape could be inhibited by the GSH

inhibitor NEM. Evidently, the nanoparticles led to apparent gene downregulation both *in vitro* and *in vivo*. When loading therapeutic siBcl2 gene into the nanoparticles, it caused significant tumor growth inhibition. After 5 times injection, the inhibition rate could achieve as high as 80%. And the expression of BCL2 protein in tumor was greatly decreased to less than 50% of the control. The crosslinking core of HA-coated particles also could achieve reduction sensitivity. Gu et al.<sup>105</sup> developed a kind of HA-shelled and core-disulfide-crosslinked biodegradable micelles for the loading of bortezomib (HA-CCMs-BP). The micelles were stable in the blood circulation, and the release significantly increased in the presence of GSH. Consequently, the micelles showed enhanced antitumor effect in the LP-1 multiple myeloma model.

Dual-stimuli responsive nanoparticles could be constructed by addition of sensitive bonds. Yin et al.<sup>106</sup> conjugated DOX to HA backbone through hydrazone and disulfide bonds, and then assembled into pH and redox dual sensitive core-shell nanoparticles. Furthermore, the nanoparticles could also physically load DOX during the assembly, resulting in extremely high drug loading capacity (about 30%). In a stimulated blood circulation environment, the 72 h DOX release from the dual sensitive nanoparticles DOX/HA-ss-DOX was only 22%. In contrast, in the presence of 20 mmol/L GSH, the release greatly increased to 82.7% in 72 h, and in the pH 5.0 without GSH, the release also increased to 67.3% in 72 h, demonstrating that the particles could response to both GSH and acidity. In combination, the release achieved 91.2% in pH 5.0 with 20 mmol/L GSH. Lin et al.<sup>107</sup> loaded DOX into MSN by hydrazone bond and then coated them with disulfide bond cross-linked HA, which also showed pH and reduction dual sensitive drug release property. In pH 5.0 and 10 mmol/L GSH, the DOX release was much faster than that in pH 5.0 + 2 µmol/L GSH and pH 7.4 + 10 mmol/L GSH, demonstrating that the release was gated by both stimuli.

### 3.6. HA as backbone of gel

Due to the biocompatibility and enzyme degradability, HA could be used for constructing gels for sustained release of cargoes in tumor<sup>108</sup>. Yang et al.<sup>109</sup> developed a methacrylation strategy to prepare HA nanogels. The copolymerization of methacrylated HA and di(ethylene glycol) diacrylate could obtain a crosslinked HA nanogel while the DOX could be loaded into the gel through simple diffusion. The DOX release showed apparent response to hyaluronidase and low pH, indicating the nanogel could specifically release drug into tumor cells.

The partially oxidized polysaccharides are good gel candidates because of the rapid degradation<sup>110</sup>. Ren et al.<sup>25</sup> prepared methacrylate-modified HA and methacrylate-modified oxidized HA as crossing precursors, then they were crosslinked in the presence of free radical initiator to form degradable gel with macroporous scaffold. The gel was then loaded with paclitaxel, R837 and combination of anti-CTLA-4 and anti-OX40 antibodies (com-ICBs) for tumor combinational therapy. When incubated the Dr-AIMS with hyaluronidase at 37 °C *in vitro*, the pore size was enlarged according to the extension of incubation time. While the degradation of the Dr-AIMS was accelerated when elevating the ratio of oxidized HA. The release of the PTX and R837 from the Dr-AIMS was almost in a linear manner, and the sustained release time depended on the ratio of oxidized HA. After partially removing tumor by surgery, the Dr-AIMS was injected into the surgical site for the treatment of the residue tumor. At day 14, the tumor weight of Dr-AIMS group was much lower than the monotherapy, the combination of R837 and PTX

and the combination of R837 and com-ICBs (Fig. 6). Furthermore, the spleen weight of Dr-AIMS group was the lowest and the survival time was longest, demonstrating the best antitumor effect of the Dr-AIMS. After mechanism evaluation, the good antitumor effect of Dr-AIMS depended on the effective depletion of M2 type macrophages and myeloid-derived suppressor cells and the enhanced infiltration of dendritic cells and effector T cells.

#### 4. Conclusions and perspective

As a natural polymer, HA has been widely used in drug delivery. In most cases, HA are used because of its potential in active tumor targeting and hyaluronidase degradation. Despite great progress in developing various HA-based formulations with superior outcomes, more attention should be paid in several other aspects. Firstly, the interaction between HA and CD44 is greatly influenced by molecular weight of HA. Secondly, the degradation by hyaluronidase may be hindered by the protein corona. In many cases, the protein corona will hinder the interaction between specific ligand and receptors<sup>11</sup>, thus similar phenomenon may occur in HA-coated nanoparticles. And the protein corona may also hinder the degradation of HA by hyaluronidase. Furthermore, surface PEG layer would also hinder the interaction between HA and hyaluronidase. Dual stimuli responsive strategy would be a good solution. The response to other stimuli, such as pH, GSH and NIR, can make the nanoparticles swell and the hyaluronidase will be easier to contact with HA. Last but not least, the hyaluronidase degradation and CD44 binding with HA may occur simultaneously in the tumor, and the cross influence should be evaluated. The CD44-mediated internalization occurs quickly when the HA-based nanoparticles bind with tumor cells, and even the fragment of HA could bind with CD44. Therefore, the hyaluronidase degradation may not significantly influence the targeting capacity of HA-based nanoparticles. Although there are several concerns to be addressed in the future research, HA is still one of the most impressive nanomaterials for constructing various DDSs, and we hope there will be one or more nanomedicines based on HA approved for clinical application.

#### Acknowledgments

The work was supported by Doctoral Research Startup Fund of the Affiliated Hospital of Southwest Medical University, China (16250), National Natural Science Foundation of China (81872806 and 31571016), Young Elite Scientists Sponsorship Program by CAST, China (2017QNRC001) and Luzhou Municipal Government-Southwest Medical University Science and Technology Strategic Cooperation Project, China (2018LZXNYPT02).

#### References

- Jain RK, Baxter LT. Mechanisms of heterogeneous distribution of monoclonal antibodies and other macromolecules in tumors: significance of elevated interstitial pressure. *Cancer Res* 1988;**48**:7022–32.
- Fang J, Nakamura H, Maeda H. The EPR effect: unique features of tumor blood vessels for drug delivery, factors involved, and limitations and augmentation of the effect. *Adv Drug Deliv Rev* 2011;**63**:136–51.
- Gao H. Progress and perspectives on targeting nanoparticles for brain drug delivery. *Acta Pharm Sin B* 2016;**6**:268–86.
- Sun Q, Zhou Z, Qiu N, Shen Y. Rational design of cancer nanomedicine: nanoproperty integration and synchronization. *Adv Mater* 2017;**29**:1606628.
- Fan W, Yung B, Huang P, Chen X. Nanotechnology for multimodal synergistic cancer therapy. *Chem Rev* 2017;**117**:13566–638.
- Shi J, Kantoff PW, Wooster R, Farokhzad OC. Cancer nanomedicine: progress, challenges and opportunities. *Nat Rev Canc* 2017;**17**:20–37.
- Weissig V, Pettinger TK, Murdock N. Nanopharmaceuticals (part 1): products on the market. *Int J Nanomed* 2014;**9**:4357–73.
- Weissig V, Guzman-Villanueva D. Nanopharmaceuticals (part 2): products in the pipeline. *Int J Nanomed* 2015;**10**:1245–57.
- Wickens JM, Alsaab HO, Kesharwani P, Bhise K, Amin M, Tekade RK, et al. Recent advances in hyaluronic acid-decorated nanocarriers for targeted cancer therapy. *Drug Discov Today* 2017;**22**:665–80.
- Schaefer L, Schaefer RM. Proteoglycans: from structural compounds to signaling molecules. *Cell Tissue Res* 2010;**339**:237–46.
- Underhill C. CD44: the hyaluronan receptor. *J Cell Sci* 1992;**103**(Pt 2):293–8.
- Swierczewska M, Han HS, Kim K, Park JH, Lee S. Polysaccharide-based nanoparticles for theranostic nanomedicine. *Adv Drug Deliv Rev* 2016;**99**:70–84.
- Kim H, Jeong H, Han S, Beack S, Hwang BW, Shin M, et al. Hyaluronate and its derivatives for customized biomedical applications. *Biomaterials* 2017;**123**:155–71.
- Dosio F, Arpicco S, Stella B, Fattal E. Hyaluronic acid for anticancer drug and nucleic acid delivery. *Adv Drug Deliv Rev* 2016;**97**:204–36.
- Seok HY, Sanoj RN, Lekshmi KM, Cherukula K, Park IK, Kim YC. CD44 targeting biocompatible and biodegradable hyaluronic acid cross-linked zein nanogels for curcumin delivery to cancer cells: *in vitro* and *in vivo* evaluation. *J Control Release* 2018;**280**:20–30.
- Mine S, Fujisaki T, Kawahara C, Tabata T, Iida T, Yasuda M, et al. Hepatocyte growth factor enhances adhesion of breast cancer cells to endothelial cells *in vitro* through up-regulation of CD44. *Exp Cell Res* 2003;**288**:189–97.
- Parayath NN, Parikh A, Amiji MM. Repolarization of Tumor-associated macrophages in a genetically engineered nonsmall cell lung cancer model by intraperitoneal administration of hyaluronic acid-based nanoparticles encapsulating microRNA-125b. *Nano Lett* 2018;**18**:3571–9.
- Chen Z, Liu M, Zhang M, Wang S, Xu L, Li C, et al. Interfering with lactate-fueled respiration for enhanced photodynamic tumor therapy by a porphyrinic MOF nanoplatfrom. *Adv Funct Mater* 2018;**28**:1803498.
- Gotov O, Battogtokh G, Ko YT. Docetaxel-loaded hyaluronic acid–cathepsin B-cleavable-peptide-gold nanoparticles for the treatment of cancer. *Mol Pharm* 2018;**15**:4668–76.
- Zhang M, Xu C, Wen L, Han MK, Xiao B, Zhou J, et al. A hyaluronidase-responsive nanoparticle-based drug delivery system for targeting colon cancer cells. *Cancer Res* 2016;**76**:7208–18.
- Liu R, Xiao W, Hu C, Xie R, Gao H. Theranostic size-reducible and no donor conjugated gold nanocluster fabricated hyaluronic acid nanoparticle with optimal size for combinational treatment of breast cancer and lung metastasis. *J Control Release* 2018;**278**:127–39.
- Zhang L, Gao S, Zhang F, Yang K, Ma Q, Zhu L. Activatable hyaluronic acid nanoparticle as a theranostic agent for optical/photoacoustic image-guided photothermal therapy. *ACS Nano* 2014;**8**:12250–8.
- Miyazaki M, Yuba E, Hayashi H, Harada A, Kono K. Hyaluronic acid-based pH-sensitive polymer-modified liposomes for cell-specific intracellular drug delivery systems. *Bioconjug Chem* 2018;**29**:44–55.
- Yin T, Liu J, Zhao Z, Zhao Y, Dong L, Yang M, et al. Redox sensitive hyaluronic acid-decorated graphene oxide for photothermally controlled tumor-cytoplasm-selective rapid drug delivery. *Adv Funct Mater* 2017;**27**:1604620.

25. Ren L, Lim YT. Degradation-regulatable architected implantable macroporous scaffold for the spatiotemporal modulation of immunosuppressive microenvironment and enhanced combination cancer immunotherapy. *Adv Funct Mater* 2018;**28**:1804490.
26. Suh KY, Khademhosseini A, Yang JM, Eng G, Langer R. Soft lithographic patterning of hyaluronic acid on hydrophilic substrates using molding and printing. *Adv Mater* 2004;**16**:584–8.
27. Gao H, He Q. The interaction of nanoparticles with plasma proteins and the consequent influence on nanoparticles behavior. *Expert Opin Drug Deliv* 2014;**11**:409–20.
28. Nel AE, Madler L, Velegol D, Xia T, Hoek EM, Somasundaran P, et al. Understanding biophysicochemical interactions at the nano-bio interface. *Nat Mater* 2009;**8**:543–57.
29. Xiao W, Xiong J, Zhang S, Xiong Y, Zhang H, Gao H. Influence of ligands property and particle size of gold nanoparticles on the protein adsorption and corresponding targeting ability. *Int J Pharm* 2018;**538**:105–11.
30. Zhang H, Wu T, Yu W, Ruan S, He Q, Gao H. Ligand size and conformation affect the behavior of nanoparticles coated with *in vitro* and *in vivo* protein corona. *ACS Appl Mater Interfaces* 2018;**10**:9094–103.
31. Aggarwal P, Hall JB, McLeland CB, Dobrovolskaia MA, McNeil SE. Nanoparticle interaction with plasma proteins as it relates to particle biodistribution, biocompatibility and therapeutic efficacy. *Adv Drug Deliv Rev* 2009;**61**:428–37.
32. Kolata A, Baradia D, Patil S, Vhora I, Kore G, Misra A. PEG—a versatile conjugating ligand for drugs and drug delivery systems. *J Control Release* 2014;**192C**:67–81.
33. Almalik A, Benabdelkamel H, Masood A, Alanazi IO, Alradwan I, Majrashi MA, et al. Hyaluronic acid coated chitosan nanoparticles reduced the immunogenicity of the formed protein corona. *Sci Rep* 2017;**7**:10542.
34. Stern R, Jedrzejak MJ. Hyaluronidases: their genomics, structures, and mechanisms of action. *Chem Rev* 2006;**106**:818–39.
35. Itano N, Kimata K. Altered hyaluronan biosynthesis in cancer progression. *Semin Canc Biol* 2008;**18**:268–74.
36. Misra S, Heldin P, Hascall VC, Karamanos NK, Skandalis SS, Markwald RR, et al. Hyaluronan–CD44 interactions as potential targets for cancer therapy. *FEBS J* 2011;**278**:1429–43.
37. Wu M, Cao M, He Y, Liu Y, Yang C, Du Y, et al. A novel role of low molecular weight hyaluronan in breast cancer metastasis. *FASEB J* 2015;**29**:1290–8.
38. Gunthert U, Hofmann M, Rudy W, Reber S, Zoller M, Haussmann I, et al. A new variant of glycoprotein CD44 confers metastatic potential to rat carcinoma cells. *Cell* 1991;**65**:13–24.
39. Zoller M. CD44: can a cancer-initiating cell profit from an abundantly expressed molecule?. *Ilular matrix receptor functions affect tumor susceptibility and progres.* *Nat Rev Canc* 2011;**11**:254–67.
40. Jaggupilli A, Elkord E. Significance of CD44 and CD24 as cancer stem cell markers: an enduring ambiguity. *Clin Dev Immunol* 2012;**2012**:708036.
41. Su J, Xu XH, Huang Q, Lu MQ, Li DJ, Xue F, et al. Identification of cancer stem-like CD44<sup>+</sup> cells in human nasopharyngeal carcinoma cell line. *Arch Med Res* 2011;**42**:15–21.
42. Leung EL, Fiscus RR, Tung JW, Tin VP, Cheng LC, Sihoe AD, et al. Non-small cell lung cancer cells expressing CD44 are enriched for stem cell-like properties. *PLoS One* 2010;**5**:e14062.
43. Okada H, Kohanbash G, Lotze MT. MicroRNAs in immune regulation—opportunities for cancer immunotherapy. *Int J Biochem Cell Biol* 2010;**42**:1256–61.
44. He XY, Liu BY, Xu C, Zhuo RX, Cheng SX. A multi-functional macrophage and tumor targeting gene delivery system for the regulation of macrophage polarity and reversal of cancer immunoresistance. *Nanoscale* 2018;**10**:15578–87.
45. Telmer PG, Tolg C, McCarthy JB, Turley EA. How does a protein with dual mitotic spindle and extracellular matrix receptor functions affect tumor susceptibility and progression?. *Commun Integr Biol* 2011;**4**:182–5.
46. Gust KM, Hofer MD, Perner SR, Kim R, Chinnaiyan AM, Varambally S, et al. RHAMM (CD168) is overexpressed at the protein level and may constitute an immunogenic antigen in advanced prostate cancer disease. *Neoplasia* 2009;**11**:956–63.
47. Shigeishi H, Fujimoto S, Hiraoka M, Ono S, Taki M, Ohta K, et al. Overexpression of the receptor for hyaluronan-mediated motility, correlates with expression of microtubule-associated protein in human oral squamous cell carcinomas. *Int J Oncol* 2009;**34**:1565–71.
48. Pandey MS, Weigel PH. A hyaluronan receptor for endocytosis (HARE) link domain *N*-glycan is required for extracellular signal-regulated kinase (ERK) and nuclear factor-kappaB (NF-kappaB) signaling in response to the uptake of hyaluronan but not heparin, dermatan sulfate, or acetylated low density lipoprotein (LDL). *J Biol Chem* 2014;**289**:21807–17.
49. Pandey MS, Baggenstoss BA, Washburn J, Harris EN, Weigel PH. The hyaluronan receptor for endocytosis (HARE) activates NF-kappaB-mediated gene expression in response to 40–400-kDa, but not smaller or larger, hyaluronans. *J Biol Chem* 2013;**288**:14068–79.
50. Girish KS, Kemparaju K. The magic glue hyaluronan and its eraser hyaluronidase: a biological overview. *Life Sci* 2007;**80**:1921–43.
51. McAttee CO, Barycki JJ, Simpson MA. Emerging roles for hyaluronidase in cancer metastasis and therapy. *Adv Cancer Res* 2014;**123**:1–34.
52. Bertrand P, Girard N, Duval C, D'Anjou J, Chauzy C, Menard JF, et al. Increased hyaluronidase levels in breast tumor metastases. *Int J Cancer* 1997;**73**:327–31.
53. Lokeshwar VB, Rubinowicz D, Schroeder GL, Forgacs E, Minna JD, Block NL, et al. Stromal and epithelial expression of tumor markers hyaluronic acid and HYAL1 hyaluronidase in prostate cancer. *J Biol Chem* 2001;**276**:11922–32.
54. Delpech B, Laquerriere A, Maingonnat C, Bertrand P, Freger P. Hyaluronidase is more elevated in human brain metastases than in primary brain tumours. *Anticancer Res* 2002;**22**:2423–7.
55. Tan JX, Wang XY, Li HY, Su XL, Wang L, Ran L, et al. HYAL1 overexpression is correlated with the malignant behavior of human breast cancer. *Int J Cancer* 2011;**128**:1303–15.
56. De Stefano I, Battaglia A, Zannoni GF, Prisco MG, Fattorossi A, Travaglia D, et al. Hyaluronic acid–paclitaxel: effects of intraperitoneal administration against CD44<sup>+</sup> human ovarian cancer xenografts. *Cancer Chemother Pharmacol* 2011;**68**:107–16.
57. Banzato A, Rondina M, Melendez-Alafort L, Zangoni E, Nadali A, Renier D, et al. Biodistribution imaging of a paclitaxel–hyaluronan bioconjugate. *Nucl Med Biol* 2009;**36**:525–33.
58. Vogus DR, Evans MA, Pusuluri A, Barajas A, Zhang M, Krishnan V, et al. A hyaluronic acid conjugate engineered to synergistically and sequentially deliver gemcitabine and doxorubicin to treat triple negative breast cancer. *J Control Release* 2017;**267**:191–202.
59. Lv Y, Xu C, Zhao X, Lin C, Yang X, Xin X, et al. Nanoplatfrom assembled from a CD44-targeted prodrug and smart liposomes for dual targeting of tumor microenvironment and cancer cells. *ACS Nano* 2018;**12**:1519–36.
60. Zhang H, Li Q, Liu R, Zhang X, Li Z, Luan Y. A versatile prodrug strategy to *in situ* encapsulate drugs in MOF nanocarriers: a case of cytarabine-IR820 prodrug encapsulated ZIF-8 toward chemophotothermal therapy. *Adv Funct Mater* 2018;**28**:1802830.
61. Wang YY, Wang WL, Shen XC, Zhou B, Chen T, Guo ZX, et al. Combination-responsive MoO<sub>3</sub>-x-hybridized hyaluronic acid hollow nanospheres for cancer phototheranostics. *ACS Appl Mater Interfaces* 2018;**10**:42088–101.
62. Wang J, Pang X, Tan X, Song Y, Liu L, You Q, et al. A triple-synergistic strategy for combinational photo/radiotherapy and multi-modality imaging based on hyaluronic acid-hybridized poly-aniline-coated WS<sub>2</sub> nanodots. *Nanoscale* 2017;**9**:5551–64.
63. Shen H, Shi S, Zhang Z, Gong T, Sun X. Coating solid lipid nanoparticles with hyaluronic acid enhances antitumor activity against melanoma stem-like cells. *Theranostics* 2015;**5**:755–71.
64. Marengo A, Forciniti S, Dando I, Dalla PE, Stella B, Tsapis N, et al. Pancreatic cancer stem cell proliferation is strongly inhibited by

- diethyldithiocarbamate–copper complex loaded into hyaluronic acid decorated liposomes. *Biochim Biophys Acta Gen Subj* 2019;**1863**: 61–72.
65. An X, Sarmiento C, Tan T, Zhu H. Regulation of multidrug resistance by microRNAs in anti-cancer therapy. *Acta Pharm Sin B* 2017;**7**:38–51.
66. Gaio E, Conte C, Esposito D, Miotto G, Quaglia F, Moret F, et al. Co-delivery of docetaxel and disulfonate tetraphenyl chlorin in one nanoparticle produces strong synergism between chemo- and photodynamic therapy in drug-sensitive and -resistant cancer cells. *Mol Pharm* 2018;**15**:4599–611.
67. Dintaman JM, Silverman JA. Inhibition of P-glycoprotein by D-alpha-tocopheryl polyethylene glycol 1000 succinate (TPGS). *Pharm Res (N Y)* 1999;**16**:1550–6.
68. Zhang X, He F, Xiang K, Zhang J, Xu M, Long P, et al. CD44-targeted facile enzymatic activatable chitosan nanoparticles for efficient antitumor therapy and reversal of multidrug resistance. *Bio-macromolecules* 2018;**19**:883–95.
69. Li B, Xu Q, Li X, Zhang P, Zhao X, Wang Y. Redox-responsive hyaluronic acid nanogels for hyperthermia-assisted chemotherapy to overcome multidrug resistance. *Carbohydr Polym* 2019;**203**: 378–85.
70. Perez-Escuredo J, Van Hee VF, Sboarina M, Falces J, Payen VL, Pellerin L, et al. Monocarboxylate transporters in the brain and in cancer. *Biochim Biophys Acta* 2016;**1863**:2481–97.
71. Sonveaux P, Vegran F, Schroeder T, Wergin MC, Verrax J, Rabbani ZN, et al. Targeting lactate-fueled respiration selectively kills hypoxic tumor cells in mice. *J Clin Invest* 2008;**118**:3930–42.
72. Chen Z, Li Z, Wang J, Ju E, Zhou L, Ren J, et al. A multi-synergistic platform for sequential irradiation-activated high-performance apoptotic cancer therapy. *Adv Funct Mater* 2014;**24**:522–9.
73. He H, Chen Y, Li Y, Song Z, Zhong Y, Zhu R, et al. Effective and selective anti-cancer protein delivery via all-functions-in-one nano-carriers coupled with visible light-responsive, reversible protein engineering. *Adv Funct Mater* 2018;**28**:1706710.
74. Cun X, Ruan S, Chen J, Zhang L, Li J, He Q, et al. A dual strategy to improve the penetration and treatment of breast cancer by combining shrinking nanoparticles with collagen depletion by losartan. *Acta Biomater* 2016;**31**:186–96.
75. Decuzzi P, Godin B, Tanaka T, Lee SY, Chiappini C, Liu X, et al. Size and shape effects in the biodistribution of intravascularly injected particles. *J Control Release* 2010;**141**:320–7.
76. Tang L, Yang X, Yin Q, Cai K, Wang H, Chaudhury I, et al. Investigating the optimal size of anticancer nanomedicine. *Proc Natl Acad Sci U S A* 2014;**111**:15344–9.
77. Kibria G, Hatakeyama H, Ohga N, Hida K, Harashima H. The effect of liposomal size on the targeted delivery of doxorubicin to integrin alpha v beta 3-expressing tumor endothelial cells. *Biomaterials* 2013;**34**:5617–27.
78. Hickey JW, Santos JL, Williford JM, Mao HQ. Control of polymeric nanoparticle size to improve therapeutic delivery. *J Control Release* 2015;**219**:536–47.
79. Xiao W, Ruan S, Yu W, Wang R, Hu C, Liu R, et al. Normalizing tumor vessels to increase the Enzyme-induced retention and targeting of gold nanoparticle for breast cancer imaging and treatment. *Mol Pharm* 2017;**14**:3489–98.
80. Ruan S, Hu C, Tang X, Cun X, Xiao W, Shi K, et al. Increased gold nanoparticle retention in brain tumors by *in situ* enzyme-induced aggregation. *ACS Nano* 2016;**10**:10086–98.
81. Shen S, Li HJ, Chen KG, Wang YC, Yang XZ, Lian ZX, et al. Spatial targeting of tumor-associated macrophages and tumor cells with a pH-sensitive cluster nanocarrier for cancer chemoimmunotherapy. *Nano Lett* 2017;**17**:3822–9.
82. Wei Q, Chen Y, Ma X, Ji J, Qiao Y, Zhou B, et al. High-efficient clearable nanoparticles for multi-modal imaging and image-guided cancer therapy. *Adv Funct Mater* 2018;**28**:1704634.
83. Ruan S, Cao X, Cun X, Hu G, Zhou Y, Zhang Y, et al. Matrix metalloproteinase-sensitive size-shrinkable nanoparticles for deep tumor penetration and pH triggered doxorubicin release. *Bio-materials* 2015;**60**:100–10.
84. Li W, Yi X, Liu X, Zhang Z, Fu Y, Gong T. Hyaluronic acid ion-pairing nanoparticles for targeted tumor therapy. *J Control Release* 2016;**225**:170–82.
85. Cadete A, Jose Alonso M. Targeting cancer with hyaluronic acid-based nanocarriers: recent advances and translational perspectives. *Nanomedicine* 2016;**11**:2341–57.
86. Liu R, Hu C, Yang Y, Zhang J, Gao H. Theranostic nanoparticles with tumor-specific enzyme-triggered size reduction and drug release to perform photothermal therapy for breast cancer treatment. *Acta Pharm Sin B* 2019;**9**:410–20.
87. Qin L, Gao H. The application of nitric oxide delivery in nanoparticle-based tumor targeting drug delivery and treatment. *Asian J Pharm Sci* 2018;**14**:66–74.
88. Hu C, Cun X, Ruan S, Liu R, Xiao W, Yang X, et al. Enzyme-triggered size shrink and laser-enhanced NO release nanoparticles for deep tumor penetration and combination therapy. *Biomaterials* 2018;**168**:64–75.
89. Hu C, Yang X, Liu R, Ruan S, Zhou Y, Xiao W, et al. Coadministration of iRGD with multistage responsive nanoparticles enhanced tumor targeting and penetration abilities for breast cancer therapy. *ACS Appl Mater Interfaces* 2018;**10**: 22571–9.
90. Cun X, Chen J, Ruan S, Zhang L, Wan J, He Q, et al. A novel strategy through combining iRGD peptide with tumor-microenvironment-responsive and multistage nanoparticles for deep tumor penetration. *ACS Appl Mater Interfaces* 2015;**7**: 27458–66.
91. Ruan S, Xiao W, Hu C, Zhang H, Rao J, Wang S, et al. Ligand-mediated and enzyme-directed precise targeting and retention for the enhanced treatment of glioblastoma. *ACS Appl Mater Interfaces* 2017;**9**:20348–60.
92. Ruan S, He Q, Gao H. Matrix metalloproteinase triggered size-shrinkable gelatin–gold fabricated nanoparticles for tumor micro-environment sensitive penetration and diagnosis of glioma. *Nano-scale* 2015;**7**:9487–96.
93. Han M, Huang-Fu MY, Guo WW, Guo NN, Chen J, Liu HN, et al. MMP-2-sensitive HA end-conjugated poly(amidoamine) dendrimers via click reaction to enhance drug penetration into solid tumor. *ACS Appl Mater Interfaces* 2017;**9**:42459–70.
94. Han HS, Choi KY, Lee H, Lee M, An JY, Shin S, et al. Gold-nanoclustered hyaluronan nano-assemblies for photothermally maneuvered photodynamic tumor ablation. *ACS Nano* 2016;**10**: 10858–68.
95. Ruan S, Yuan M, Zhang L, Hu G, Chen J, Cun X, et al. Tumor microenvironment sensitive doxorubicin delivery and release to glioma using angiopep-2 decorated gold nanoparticles. *Biomaterials* 2015;**37**:425–35.
96. Lee ES, Gao Z, Bae YH. Recent progress in tumor pH targeting nanotechnology. *J Control Release* 2008;**132**:164–70.
97. Ding L, Jiang Y, Zhang J, Klok HA, Zhong Z. PH-sensitive coiled-coil peptide-cross-linked hyaluronic acid nanogels: synthesis and targeted intracellular protein delivery to CD44 positive cancer cells. *Biomacromolecules* 2018;**19**:555–62.
98. Xia J, Du Y, Huang L, Chaurasiya B, Tu J, Webster TJ, et al. Redox-responsive micelles from disulfide bond-bridged hyaluronic acid-tocopherol succinate for the treatment of melanoma. *Nano-medicine-Uk* 2018;**14**:713–23.
99. Du X, Yin S, Zhou F, Du X, Xu J, Gu X, et al. Reduction-sensitive mixed micelles for selective intracellular drug delivery to tumor cells and reversal of multidrug resistance. *Int J Pharm* 2018;**550**:1–13.

100. Cai Z, Zhang H, Wei Y, Wei Y, Xie Y, Cong F. Reduction- and pH-sensitive hyaluronan nanoparticles for delivery of iridium (III) anti-cancer drugs. *Biomacromolecules* 2017;**18**:2102–17.
101. Debele TA, Yu LY, Yang CS, Shen YA, Lo CL. PH- and GSH-sensitive hyaluronic acid–MP conjugate micelles for intracellular delivery of doxorubicin to colon cancer cells and cancer stem cells. *Biomacromolecules* 2018;**19**:3725–37.
102. Song Y, Cai H, Yin T, Huo M, Ma P, Zhou J, et al. Paclitaxel-loaded redox-sensitive nanoparticles based on hyaluronic acid–vitamin E succinate conjugates for improved lung cancer treatment. *Int J Nanomed* 2018;**13**:1585–600.
103. Tian C, Asghar S, Xu Y, Chen Z, Zhang J, Ping Q, et al. Tween 80-modified hyaluronic acid–ss-curcumin micelles for targeting glioma: synthesis, characterization and their *in vitro* evaluation. *Int J Biol Macromol* 2018;**120**:2579–88.
104. Zhou Z, Li H, Wang K, Guo Q, Li C, Jiang H, et al. Bioreducible cross-linked hyaluronic acid/calcium phosphate hybrid nanoparticles for specific delivery of siRNA in melanoma tumor therapy. *ACS Appl Mater Interfaces* 2017;**9**:14576–89.
105. Gu Z, Wang X, Cheng R, Cheng L, Zhong Z. Hyaluronic acid shell and disulfide-crosslinked core micelles for *in vivo* targeted delivery of bortezomib for the treatment of multiple myeloma. *Acta Biomater* 2018;**80**:288–95.
106. Yin T, Wang Y, Chu X, Fu Y, Wang L, Zhou J, et al. Free adriamycin-loaded pH/reduction dual-responsive hyaluronic acid–adriamycin prodrug micelles for efficient cancer therapy. *ACS Appl Mater Interfaces* 2018;**10**:35693–704.
107. Lin JT, Du JK, Yang YQ, Li L, Zhang DW, Liang CL, et al. pH and redox dual stimulate-responsive nanocarriers based on hyaluronic acid coated mesoporous silica for targeted drug delivery. *Mater Sci Eng C Mater Biol Appl* 2017;**81**:478–84.
108. Burdick JA, Prestwich GD. Hyaluronic acid hydrogels for biomedical applications. *Adv Mater* 2011;**23**:H41–56.
109. Yang C, Wang X, Yao X, Zhang Y, Wu W, Jiang X. Hyaluronic acid nanogels with enzyme-sensitive cross-linking group for drug delivery. *J Control Release* 2015;**205**:206–17.
110. Verbeke CS, Mooney DJ. Injectable, pore-forming hydrogels for *in vivo* enrichment of immature dendritic cells. *Adv Healthc Mater* 2015;**4**:2677–87.
111. Xiao W, Gao H. The impact of protein corona on the behavior and targeting capability of nanoparticle-based delivery system. *Int J Pharm* 2018;**552**:328–39.